

SAFR: Neuron Redistribution for Interpretability

Ruidi Chang Chunyuan Deng Hanjie Chen

Department of Computer Science

Rice University

{ruidi.chang, hanjie}@rice.edu

Abstract

Superposition refers to encoding representations of multiple features within a single neuron, which is common in transformers. This property allows neurons to combine and represent multiple features, enabling the model to capture intricate information and handle complex tasks. Despite promising performance, the model’s interpretability has been diminished. This paper presents a novel approach to enhance transformer interpretability by regularizing feature superposition. We introduce SAFR¹, which simply applies regularizations to the loss function to promote monosemantic representations for important tokens while encouraging polysemanticity for correlated token pairs, where important tokens and correlated token pairs are identified via VMASK (Chen and Ji, 2020) and attention weights. With a transformer model on two classification tasks, SAFR improves interpretability without compromising prediction performance. Given an input to the model, SAFR provides an explanation by visualizing the neuron allocation and interaction within the MLP layers.

1 Introduction

Individual neurons in neural networks can represent multiple features from the input. This phenomenon, known as superposition, improves the model’s ability to capture intricate relationships between features (Olah et al., 2020) and complicates the understanding of the underlying processes behind the model’s decision-making (Elhage et al., 2022). Facing these challenges, recent research like sparse autoencoders (SAEs) (Huben et al., 2024) artificially decomposes the representation space into a sparse vector space through auxiliary networks. However, while SAEs provide a method to *interpret* features through combinations of sparse activations, there is still a lack of sufficient research on *controlling* neuron distribution.

In this paper, we ask the question: *Can we enhance model interpretability by explicitly controlling the distribution of features across neurons?* An intuitive approach is to encourage the development of monosemantic neurons (Elhage et al., 2022; Bricken et al., 2023; Wang et al., 2024) by regulating activations. However, focusing solely on monosemanticity may limit the model’s ability to capture feature interactions, potentially hindering overall performance.

To address this challenge, we propose a novel method called **Superposition-Aware Feature Regularization** (SAFR) to enhance model interpretability by strategically reallocating neurons through a modified loss function, approached from two perspectives. As illustrated in Figure 1, our framework incorporates regularization techniques aimed at promoting monosemantic representations for important tokens, while simultaneously fostering polysemanticity among correlated token pairs. The identification of important tokens is achieved via a variational inference network, adapted from VMASK (Chen and Ji, 2020). Additionally, correlated token pairs are identified based on attention weights to foster polysemantic representation.

We evaluate SAFR on the SST-2 (Socher et al., 2013) and IMDB (Maas et al., 2011) datasets to assess its effectiveness. When the top 30% of words identified by SAFR are removed, we observe a significant drop in test accuracy—18.24% on SST-2 and 27.04% on IMDB. As we incrementally remove additional tokens, the accuracy continues to decline in a consistent manner. To further substantiate these findings, we visualize the neuron allocation within the FFN layers of a transformer block. Our experimental results confirm that SAFR can efficiently reallocate feature distributions across neurons while preserving a reasonable degree of polysemanticity, significantly improving interpretability in transformers while maintaining performance at comparable levels.

¹SAFR: Superposition-Aware Feature Regularization

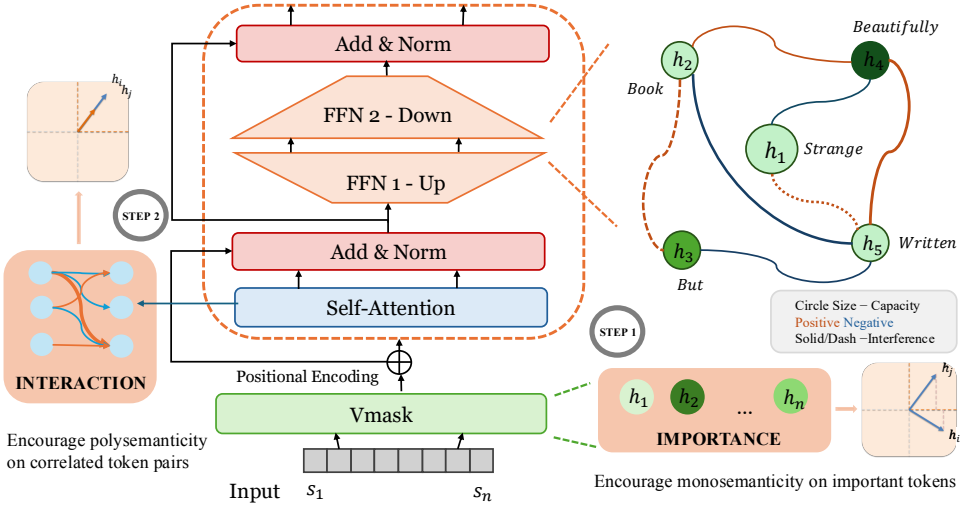


Figure 1: **Basic structure of SAFR.** i) Promote monosemanticity for important tokens after the embedding layers. ii) Leverage the attention mechanism to enhance polysemanticity among correlated token pairs.

2 Preliminaries

Given an input sequence of n tokens $S = \langle s_1, \dots, s_n \rangle$ and a transformer $f(\cdot)$ with L layers, let h_i^ℓ denote the hidden representation obtained at layer $\ell \in [1, \dots, L]$ and position $i \in [1, \dots, n]$. Following previous work (Scherlis et al., 2022; Elhage et al., 2022), we define *interference*, *polysemanticity*, and *capacity* as follows.

Interference The *interference* (I) measures the overlap or similarity between the two representations at the same layer:

$$I_{i,j}^\ell = (h_i^\ell \cdot h_j^\ell)^2 \quad (1)$$

Interference quantifies how much the hidden representations interfere with or influence each other. Higher interference means more overlap, suggesting the tokens share representational dimensions.

Polysemanticity The *polysemanticity* (P) describes the extent to which a single hidden representation captures information from multiple tokens:

$$P_i^\ell = \sum_{j \neq i} (\hat{h}_i^\ell \cdot h_j^\ell)^2 \quad (2)$$

Here, \hat{h}_i^ℓ denotes the normalized representation of h_i^ℓ (excluding its own magnitude). A high polysemanticity value indicates that a single dimension is “polysemantic”, meaning it represents information from multiple tokens simultaneously.

Capacity The *capacity* (C) quantifies how much of a hidden representation is dedicated to representing token i :

$$C_i^\ell = \frac{(h_i^\ell \cdot h_i^\ell)^2}{\sum_j (h_i^\ell \cdot h_j^\ell)^2} \quad (3)$$

where $0 \leq C_i \leq 1$ and $1 \leq C \leq D$, D denotes the hidden dimension size. A higher capacity value indicates that the representation at position i is more focused on its own token.

3 Methodology

SAFR aims to enhance the interpretability of models by strategically reallocating neurons using superposition regularization strategy.

The baseline is defined via original model in cross-entropy loss $\mathcal{L}_{\text{CE}} = -\frac{1}{M} \sum_{m=1}^M \sum_{g=1}^G y_m^g \log(\hat{y}_m^g)$, where M is the number of samples in the dataset and G is the number of classes in text classification. To improve model efficiency and interpretability in a constrained space, we propose a two-part regularization: one promotes monosemantic representations for important tokens, while the other encourages polysemanticity for correlated token pairs to reduce redundancy.

The proposed loss function integrates these regularization terms accordingly:

$$\mathcal{L} = \mathcal{L}_{\text{CE}} + \lambda_{\text{Imp}} \cdot \mathcal{L}_{\text{Importance}} + \lambda_{\text{Inter}} \cdot \mathcal{L}_{\text{Interaction}}$$

where λ_{Imp} controls the importance loss term and λ_{Inter} controls the interaction loss term.

Model	SST-2				IMDB			
	Acc _S	Acc _{̄S(r)}	Acc _{̄S(k)}	SRS	Acc _S	Acc _{̄S(r)}	Acc _{̄S(k)}	SRS
Baseline	71.81	75.81	74.96	-3.15	80.88	74.31	76.92	3.96
$\lambda_{Imp} = 0, \lambda_{Inter} = 0$	71.24	71.98	61.98	9.26	79.07	73.30	64.70	14.37
SAFR	72.96	75.3	54.72	18.24	78.23	74.52	51.19	27.04

Table 1: Evaluation on SST-2 and IMDB datasets, $k = 30$. Acc_S denotes prediction accuracy for original test dataset. $Acc_{\bar{S}(r)}$ denotes prediction accuracy for dataset randomly drop $k\%$ words. $Acc_{\bar{S}(k)}$ denotes prediction accuracy for deleting $k\%$ words based on capacity. SAFR achieves a SRS score of 18.24 for SST-2 and 27.04 for IMDB, outperforming the baseline model, indicating an improvement on model interpretability.

Importance-Based Regularization We apply the VMASK (Chen and Ji, 2020) between the embedding layer and the positional encoder to identify important tokens. VMASK (Chen and Ji, 2020) is a variational word mask layer that is inserted into a neural text classifier and trained with the model. It learns to limit the flow of globally irrelevant or noisy word-level feature information to subsequent network layers, thus forcing the model to focus on the important features for prediction. To encourage monosemanticity for important tokens, we introduce a regularization term $\mathcal{L}_{Importance} = \sum_{i=1}^T \sqrt{P_i^V/E}$, where T is the maximum token length, E represents the embedding dimension and P_i^V denotes the polysemanticity for the hidden representation of the i -th token in the VMASK layer. This regularization term penalize important tokens with high polysemanticity.

Interaction-Based Regularization We leverage the attention mechanism and employ the attention weights to identify correlated tokens. The α -th self-attention head is described as follows:

$$A_\alpha = \text{softmax} \left(\frac{Q_\alpha K_\alpha^T}{\sqrt{d_k}} \right)$$

where $Q_\alpha = \mathbf{X}W_\alpha^Q$ and $K_\alpha = \mathbf{X}W_\alpha^K$, with $Q_\alpha, K_\alpha \in \mathbb{R}^{n \times d_k}$. $\mathbf{X} = E_{\text{pos}}(S')$ denotes the input matrix to the attention layer, where $E_{\text{pos}}(S')$ is the positional encoding applied to the output S' from the vmask layer. The score $A_{\alpha(i,j)}$ indicates how much attention token i places on token j .

To encourage pairs of highly correlated features to exhibit high polysemanticity, we introduce a loss term $\mathcal{L}_{Interaction} = \sum_\alpha \sum_{i,j} \frac{1}{T^2} A_{\alpha(i,j)} \cdot (1 - I_{i,j}^{A_\alpha})$, where $I_{i,j}^{A_\alpha}$ is the *Interference* of the attention weights metric of the α -th attention head. This loss term penalizes highly correlated features that exhibit low interference values.

Proposed Loss Function The loss term is now defined as:

$$\begin{aligned} \mathcal{L} &= \mathcal{L}_{CE} + \lambda_{Imp} \cdot \mathcal{L}_{Importance} + \lambda_{Inter} \cdot \mathcal{L}_{Interaction} \\ &= - \sum_{m=1}^M \sum_{g=1}^G y_m^g \log(\hat{y}_m^g) + \lambda_{Imp} \cdot \sum_{m=1}^M \sum_{i=1}^T \sqrt{P_i^V/E} \\ &\quad + \lambda_{Inter} \cdot \sum_{m=1}^M \sum_{\alpha} \sum_{i,j} \frac{1}{T^2} A_{\alpha(i,j)} (1 - I_{i,j}^{A_\alpha}) \end{aligned}$$

4 Experiment Setup

The proposed method is evaluated on two classification tasks using a standard transformer model.

Datasets We adopt 2 benchmark datasets: Stanford Sentiment Treebank binary version SST-2 (Socher et al., 2013) and movie reviews IMDB (Maas et al., 2011). Table 4 in Appendix A shows the statistics of the datasets.

Model We use a typical transformer architecture with a single layer, following the standard setup (Vaswani, 2017). This includes the complete transformer framework with its attention mechanism and positional encodings. In the multi-layer perceptron (MLP) section, we use two feed forward sub-layers: we first expand the dimensionality by a factor of four, then reduce it back by the same factor, aligning with the commonly used configuration in transformer models. The model is using random embedding to avoid the influence of embedding information. Table 5 in Appendix A shows the statistics of the model.

Baseline Since our objective is to investigate how regularization can modify neuron resource allocation to enhance interpretability, we employ a standard Transformer model, without any modifications, as the baseline for comparison.

Evaluation To evaluate our method, we define an evaluation metric called **Superposition**

Regularization Score (SRS). By deleting the top $k\%$ of tokens based on capacity, **SRS** calculates the average change in the prediction accuracy over all test data as follows:

$$SRS(k) = \frac{1}{M} \left(\sum_{S=1}^M 1 \cdot (\hat{y}_S = y) - \sum_{S=1}^M 1 \cdot (\hat{y}_{\tilde{S}^{(k)}} = y) \right)$$

where $\tilde{S}^{(k)}$ is constructed by dropping the $k\%$ top-scored words from S . The SRS metric serves to evaluate how effectively the model arranges neurons to represent features. The SRS metric quantifies the alignment between neuron allocations and the semantic significance of tokens. By assessing the structure of neuron allocation, SRS provides insights into the interpretability of the model’s internal encoding of information. Higher SRS values indicate that the deleted words are important, therefore indicates a stronger superposition regularization.

5 Results and Analysis

SAFR Improves Interpretability. Results in Table 1 demonstrate that SAFR achieves superior SRS scores of 18.24 and 27.04 for SST-2 and IMDB datasets respectively, surpassing the baseline model. This provides evidence for SAFR’s efficacy in improving interpretability. Notably, even without regularization ($\lambda_{Imp} = 0$ and $\lambda_{Inter} = 0$), the interpretability layer before the transformer block yields improved SRS scores, suggesting its influence on neuronal allocation. An ablation study of λ_{Imp} and λ_{Inter} is detailed in Table 2. When calibrating these regularization terms, two critical trade-offs emerge: Excessive emphasis λ_{Imp} may compromise the model’s ability to capture feature interactions. Conversely, focusing solely on λ_{Inter} without balancing feature importance can reduce attention to critical words. Additional ablation studies can be found in Appendix D.

Model	SST-2			
	Acc _S	Acc _{$\tilde{S}^{(r)}$}	Acc _{$\tilde{S}^{(k)}$}	SRS
Baseline	71.81	75.81	74.96	-3.15
$\lambda_{Imp} = 0, \lambda_{Inter} = 0$	71.24	71.98	61.98	9.26
$\lambda_{Imp} = 0, \lambda_{Inter} = 1$	71.98	69.07	61.86	10.12
$\lambda_{Imp} = 1, \lambda_{Inter} = 0$	71.47	72.16	55.35	16.12
$\lambda_{Imp} = 1, \lambda_{Inter} = 0.1$	72.96	75.30	54.72	18.24
$\lambda_{Imp} = 100, \lambda_{Inter} = 100$	61.46	62.04	51.06	10.40

Table 2: Ablation study of λ_{Imp} and λ_{Inter} . λ choosing influence prediction accuracy and model interpretability.

Sensitivity to k Selection. Figure 3 illustrates the effect of token removal based on capacity. The

$k\%$ top-scored words are directly removed from the original text to ensure that the evaluation reflects the model’s ability to perform with reduced input information. As tokens are incrementally removed, the accuracy declines consistently. The greater decline observed in our model compared to the baseline suggests that our model is more interpretable.

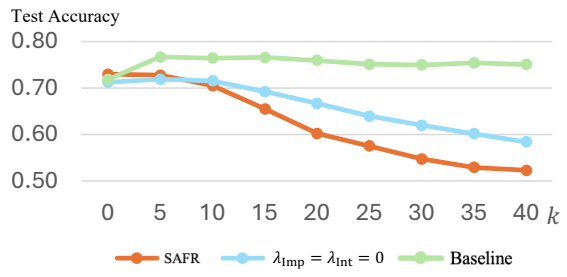


Figure 3: Sensitivity to k Selection. As tokens are incrementally removed, the accuracy declines consistently.

Average Capacity Across the Vocabulary. Table 3 presents an analysis of the average capacity per token status (important or not w.r.t VMASK) on the entire test dataset. Tokens are classified based on VMASK scores, with the top 30% identified as important and the rest 70% as less important. These results demonstrate the effectiveness of SAFR in prioritizing and allocating greater representational capacity to features that are important for tasks.

Average Capacity	SST-2	IMDB
All Tokens	0.1925	0.1372
Important Tokens	0.4141	0.2912
Less Important Tokens	0.0975	0.0712

Table 3: Average capacity metric for SST-2 and IMDB datasets. The metric reveals that important tokens exhibit significantly higher capacity scores compared to the overall average capacity.

This strategic allocation enhances the model’s ability to provide clearer and more meaningful insights into its decision-making processes, reinforcing its value as a tool for model interpretability.

Neuron Allocation Across Layers. We conducted an analysis of neuron allocation across layers, with the visualizations presented in Appendix C. Our observations reveal that neurons within the embedding layer exhibit a random distribution, failing to effectively capture their relative importance or inter-neuronal interactions. The VMASK layer begins to identify important tokens

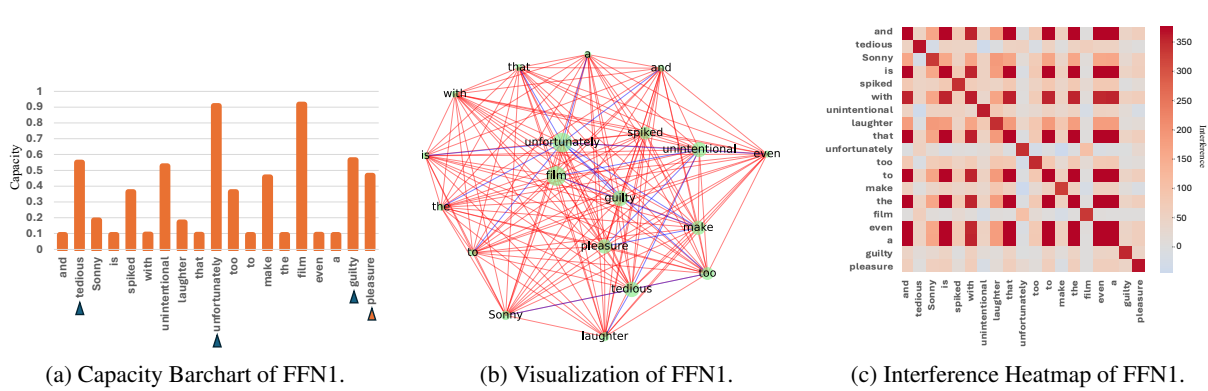


Figure 2: (a) Important words exhibit higher capacity. (b) Circle size represents feature capacity, with larger circles indicating greater capacity. Red lines denote positive correlations, blue lines indicate negative correlations, and shorter lines indicate stronger correlations. (c) Important words demonstrate lower polysemanticity, while correlated words pair exhibit relatively higher interference.

at a global level, yet it lacks the capability to analyze token-to-token interactions. While the attention layer demonstrates proficiency in capturing inter-token relationships, the interpretation of token importance remains a debatable topic. The second feedforward neural network layer compresses information into a lower-dimensional space and tends to allocate neuron capacity in a uniform manner. The expansion of the feedforward neural network, denotes FFN1 layer in our model, facilitates the network’s ability to learn more intricate patterns and relationships within the data (Elhage et al., 2021). Our observation reveals that important tokens exhibit greater monosemanticity, and correlated token pairs demonstrate higher interference, illustrated in Figure 2a and 2c.

Visualization of FFN1 Figure 2b illustrates the enhanced interpretability achieved after applying SAFR. In the visualization, the size of the circles represents the capacity of individual features, where larger circles indicate greater capacity. The red and blue lines depict interference between features, with red lines corresponding to positive correlations and blue lines indicating negative correlations. The length of these lines reflects the strength of the correlation. This representation provides a clear and intuitive understanding of both the distribution of neuron and the relationships among features, showcasing the effectiveness of SAFR in improving the interpretability of FFN1 layer. By visualizing these dynamics, the figure highlights key insights into feature importance and their interactions within the model.

6 Related Work

Superposition in neural networks has gained attention, with foundational work by (Arora et al., 2018;

Goh, 2016). Olah et al. (2020) developed this idea into the “superposition hypothesis” and initiated studies on mechanistic interpretability concerning polysemantic neurons and circuits. (Lecomte et al., 2024) showed that polysemanticity can emerge incidentally through regularization and neural noise.

Elhage et al. (2022) illustrated superposition in simplified networks. Concurrently, theoretical explorations (Scherlis et al., 2022; Henighan et al., 2023; Hänni et al., 2024; Gurnee et al., 2023; Marshall and Kirchner, 2024; Hänni et al., 2024; Katta, 2024) and applications in language models (Chen et al., 2023, 2024) have expanded the field.

Interpretability efforts include works like (Dreyer et al., 2024; Black et al., 2022; Wang et al., 2023). Challenges in lifelong knowledge editing (Hu et al., 2024) and identifying universal feature spaces across models (Lan et al., 2024) mark promising directions for future research.

7 Conclusion

In this work, we introduced SAFR, a novel approach to enhance model interpretability by strategically regularizing feature superposition. Experiments on SST-2 and IMDB show that SAFR improves interpretability, as measured by our SRS metric, without compromising prediction performance.

Our method provides insights into the relationship between superposition and interpretability in transformers and offers a framework for visualizing neuron allocation across layers. This work contributes to mechanistic interpretability and suggests promising directions for extending the approach to larger models and broader applications.

8 Limitation

This study has several limitations. First, experiments were conducted using a single-layer transformer model; future work should examine the scalability of SAFR with more complex architectures. Second, while focused on classification task, the applicability of SAFR to other NLP tasks—such as natural language inference, question answering, and text generation—remains unexplored. Third, there is a need for more comprehensive and standardized evaluation metrics to assess SAFR effectively. Finally, SAFR does not fully elucidate the causal mechanisms behind the model’s decision-making process. Addressing these challenges offers valuable opportunities for future research.

9 Ethic Statements

Our research focuses on understanding and controlling the inner workings of transformer models, without collecting or using any human data; no personal or sensitive information is handled in this study. All datasets used in this work are public.

References

Sanjeev Arora, Yuanzhi Li, Yingyu Liang, Tengyu Ma, and Andrej Risteski. 2018. [Linear algebraic structure of word senses, with applications to polysemy](#). *Transactions of the Association for Computational Linguistics*, 6:483–495.

Sid Black, Lee D. Sharkey, Léo Grinsztajn, Eric Winsor, Daniel A. Braun, Jacob Merizian, Kip Parker, Carlos Ram’on Guevara, Beren Millidge, Gabriel Alfour, and Connor Leahy. 2022. [Interpreting neural networks through the polytope lens](#). *ArXiv*, abs/2211.12312.

Trenton Bricken, Adly Templeton, Joshua Batson, Brian Chen, Adam Jermyn, Tom Conerly, Nick Turner, Cem Anil, Carson Denison, Amanda Askell, Robert Lasenby, Yifan Wu, Shauna Kravec, Nicholas Schiefer, Tim Maxwell, Nicholas Joseph, Zac Hatfield-Dodds, Alex Tamkin, Karina Nguyen, Brayden McLean, Josiah E Burke, Tristan Hume, Shan Carter, Tom Henighan, and Christopher Olah. 2023. Towards monosemanticity: Decomposing language models with dictionary learning. *Transformer Circuits Thread*. [Https://transformer-circuits.pub/2023/monosemantic-features/index.html](https://transformer-circuits.pub/2023/monosemantic-features/index.html).

Hanjie Chen and Yangfeng Ji. 2020. [Learning variational word masks to improve the interpretability of neural text classifiers](#). In *Proceedings of the 2020 Conference on Empirical Methods in Natural Language Processing (EMNLP)*, pages 4236–4251, Online. Association for Computational Linguistics.

Jiawei Chen, Hongyu Lin, Xianpei Han, Yaojie Lu, Shanshan Jiang, Bin Dong, and Le Sun. 2024. [Few-shot named entity recognition via superposition concept discrimination](#). In *Proceedings of the 2024 Joint International Conference on Computational Linguistics, Language Resources and Evaluation (LREC-COLING 2024)*, pages 7220–7231, Torino, Italia. ELRA and ICCL.

Zhongtian Chen, Edmund Lau, Jake Mendel, Susan Wei, and Daniel Murefet. 2023. [Dynamical versus bayesian phase transitions in a toy model of superposition](#). *ArXiv*, abs/2310.06301.

Maximilian Dreyer, Erblina Purelku, Johanna Vielhaben, Wojciech Samek, and Sebastian Lapuschkin. 2024. Pure: Turning polysemantic neurons into pure features by identifying relevant circuits. In *Proceedings of the IEEE/CVF Conference on Computer Vision and Pattern Recognition (CVPR) Workshops*, pages 8212–8217.

Nelson Elhage, Tristan Hume, Catherine Olsson, Nicholas Schiefer, Tom Henighan, Shauna Kravec, Zac Hatfield-Dodds, Robert Lasenby, Dawn Drain, Carol Chen, et al. 2022. Toy models of superposition. *arXiv preprint arXiv:2209.10652*.

Nelson Elhage, Neel Nanda, Catherine Olsson, Tom Henighan, Nicholas Joseph, Ben Mann, Amanda Askell, Yuntao Bai, Anna Chen, Tom Conerly, Nova DasSarma, Dawn Drain, Deep Ganguli, Zac Hatfield-Dodds, Danny Hernandez, Andy Jones, Jackson Kernion, Liane Lovitt, Kamal Ndousse, Dario Amodei, Tom Brown, Jack Clark, Jared Kaplan, Sam McCandlish, and Chris Olah. 2021. A mathematical framework for transformer circuits. *Transformer Circuits Thread*. [Https://transformer-circuits.pub/2021/framework/index.html](https://transformer-circuits.pub/2021/framework/index.html).

Gabriel Goh. 2016. [Decoding the thought vector](#).

Wes Gurnee, Neel Nanda, Matthew Pauly, Katherine Harvey, Dmitrii Troitskii, and Dimitris Bertsimas. 2023. [Finding neurons in a haystack: Case studies with sparse probing](#). *Transactions on Machine Learning Research*.

Kaarel Hänni, Jake Mendel, Dmitry Vaintrob, and Lawrence Chan. 2024. [Mathematical models of computation in superposition](#). In *ICML 2024 Workshop on Mechanistic Interpretability*.

Tom Henighan, Shan Carter, Tristan Hume, Nelson Elhage, Robert Lasenby, Stanislav Fort, Nicholas Schiefer, and Christopher Olah. 2023. Superposition, memorization, and double descent. *Transformer Circuits Thread*, 6:24.

Chenhui Hu, Pengfei Cao, Yubo Chen, Kang Liu, and Jun Zhao. 2024. [Knowledge in superposition: Unveiling the failures of lifelong knowledge editing for large language models](#). *ArXiv*, abs/2408.07413.

Robert Huben, Hoagy Cunningham, Logan Riggs Smith, Aidan Ewart, and Lee Sharkey. 2024. [Sparse autoencoders find highly interpretable features in language models](#). In *The Twelfth International Conference on Learning Representations*.

Pavan Katta. 2024. [On implications of scaling laws on feature superposition](#). *ArXiv*, abs/2407.01459.

Michael Lan, Philip Torr, Austin Meek, Ashkan Khakzar, David Krueger, and Fazl Barez. 2024. [Sparse autoencoders reveal universal feature spaces across large language models](#). *Preprint*, arXiv:2410.06981.

Victor Lecomte, Kushal Thaman, Rylan Schaeffer, Naomi Bashkansky, Trevor Chow, and Sanmi Koyejo. 2024. [What causes polysemy? an alternative origin story of mixed selectivity from incidental causes](#). In *ICLR 2024 Workshop on Representational Alignment*.

Andrew L. Maas, Raymond E. Daly, Peter T. Pham, Dan Huang, Andrew Y. Ng, and Christopher Potts. 2011. [Learning word vectors for sentiment analysis](#). In *Proceedings of the 49th Annual Meeting of the Association for Computational Linguistics: Human Language Technologies*, pages 142–150, Portland, Oregon, USA. Association for Computational Linguistics.

Simon C Marshall and Jan H Kirchner. 2024. Understanding polysemy in neural networks through coding theory. *arXiv preprint arXiv:2401.17975*.

Chris Olah, Nick Cammarata, Ludwig Schubert, Gabriel Goh, Michael Petrov, and Shan Carter. 2020. [Zoom in: An introduction to circuits](#). *Distill*. [Https://distill.pub/2020/circuits/zoom-in](https://distill.pub/2020/circuits/zoom-in).

Adam Scherlis, Kshitij Sachan, Adam S Jermyn, Joe Benton, and Buck Shlegeris. 2022. Polysemy and capacity in neural networks. *arXiv preprint arXiv:2210.01892*.

Richard Socher, Alex Perelygin, Jean Wu, Jason Chuang, Christopher D. Manning, Andrew Ng, and Christopher Potts. 2013. [Recursive deep models for semantic compositionality over a sentiment treebank](#). In *Proceedings of the 2013 Conference on Empirical Methods in Natural Language Processing*, pages 1631–1642, Seattle, Washington, USA. Association for Computational Linguistics.

A Vaswani. 2017. Attention is all you need. *Advances in Neural Information Processing Systems*.

Jiachuan Wang, Shimin Di, Lei Chen, and Charles Wang Wai Ng. 2023. [Learning from emergence: A study on proactively inhibiting the monosemantic neurons of artificial neural networks](#). In *Knowledge Discovery and Data Mining*.

Jiachuan Wang, Shimin Di, Lei Chen, and Charles Wang Wai Ng. 2024. [Learning from emergence: A study on proactively inhibiting the monosemantic neurons of artificial neural networks](#). *Preprint*, arXiv:2312.11560.

A Dataset Statistics

This section provides the statistical summary for the datasets and model.

Datasets	#Train	#Dev	#Test
SST2	6244	825	1749
IMDB	20k	5k	25k

Table 4: Summary statistics for the datasets, where # counts the number of examples in the train/dev/test sets.

Layer	Dimension
Embedding	(Input Dimension, 256)
FFN1	(256, 1024)
FFN2	(1024, 256)

Table 5: Summary statistic for the model: Layer dimensions.

B Cross Entropy Loss

Given an input sequence of n tokens $S = \langle s_1, \dots, s_n \rangle$ and a transformer $f(\cdot)$ with L layers, let h_i^ℓ denote the hidden representation obtained at layer $\ell \in [1, \dots, L]$ and position $i \in [1, \dots, n]$. Following previous work (Scherlis et al., 2022; Elhage et al., 2022), we define *interference*, *polysemy*, and *capacity* as follows. The baseline is defined via the original model using the cross-entropy loss:

$$\mathcal{L}_{\text{CE}} = -\frac{1}{M} \sum_{m=1}^M \sum_{g=1}^G y_m^g \log(\hat{y}_m^g)$$

where M is the number of samples in the dataset and G is the number of classes in text classification.

Additionally, for the input sequence S , let:

- \hat{y}_t represent the predicted probability distribution over the vocabulary at position t ,
- y_t represent the true one-hot encoded distribution for the token at position t ,
- V denote the size of the vocabulary, and
- c_t be the index of the correct token at position t .

The **cross-entropy loss** at position t is defined as:

$$\mathcal{L}_t = - \sum_{i=1}^V y_{t,i} \log(\hat{y}_{t,i})$$

Since y_t is a one-hot encoded vector, this simplifies to:

$$\mathcal{L}_t = - \log(\hat{y}_{t,c_t})$$

The total cross-entropy loss for the sequence S is the average over all tokens in the sequence:

$$\mathcal{L} = \frac{1}{n} \sum_{t=1}^n \mathcal{L}_t = - \frac{1}{n} \sum_{t=1}^n \log(\hat{y}_{t,c_t})$$

where \hat{y}_{t,c_t} is the predicted probability of the correct token at position t .

C Neuron Allocation Across Layers

This section presents the observations regarding neuron allocation across the various layers.

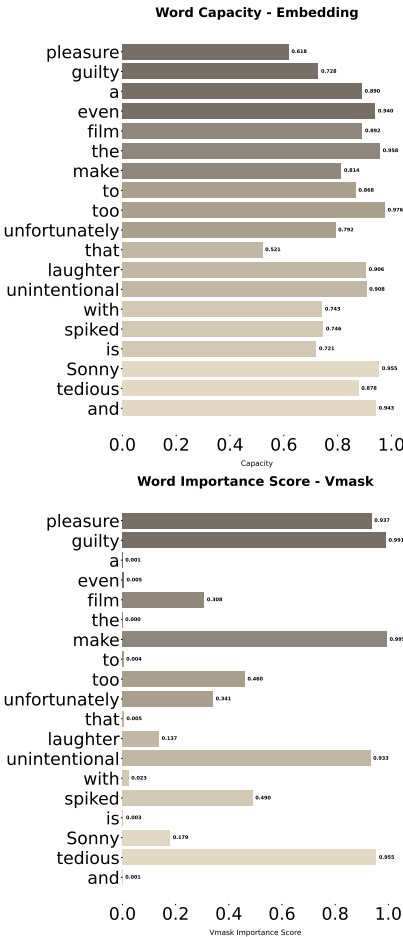


Figure 4: Cross Layers Output-1: Capacity. Capacity for FFN1 is interpretable.

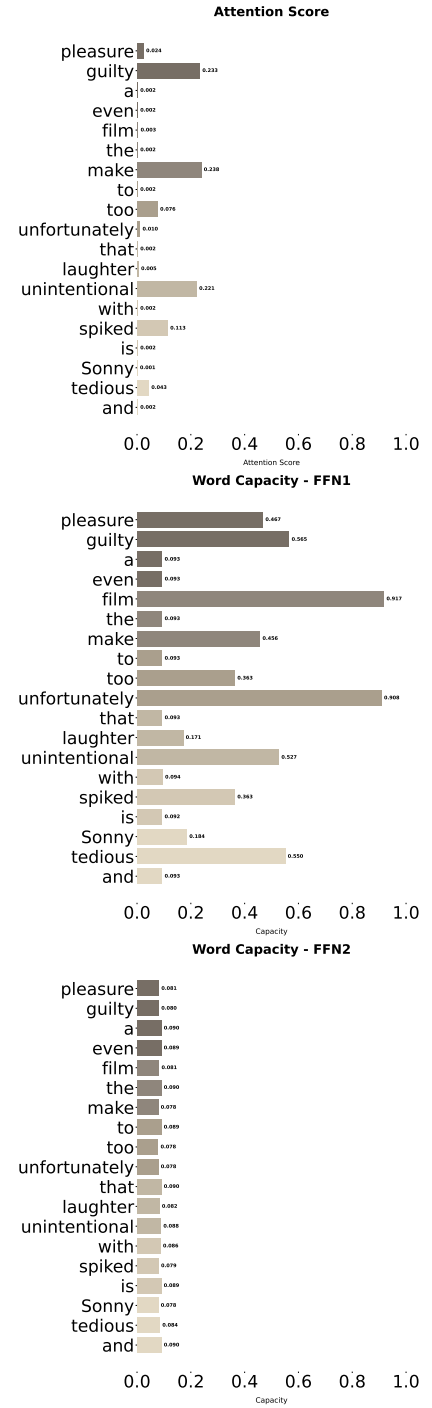


Figure 5: Cross Layers Output-2: Capacity. Capacity for FFN1 is interpretable.

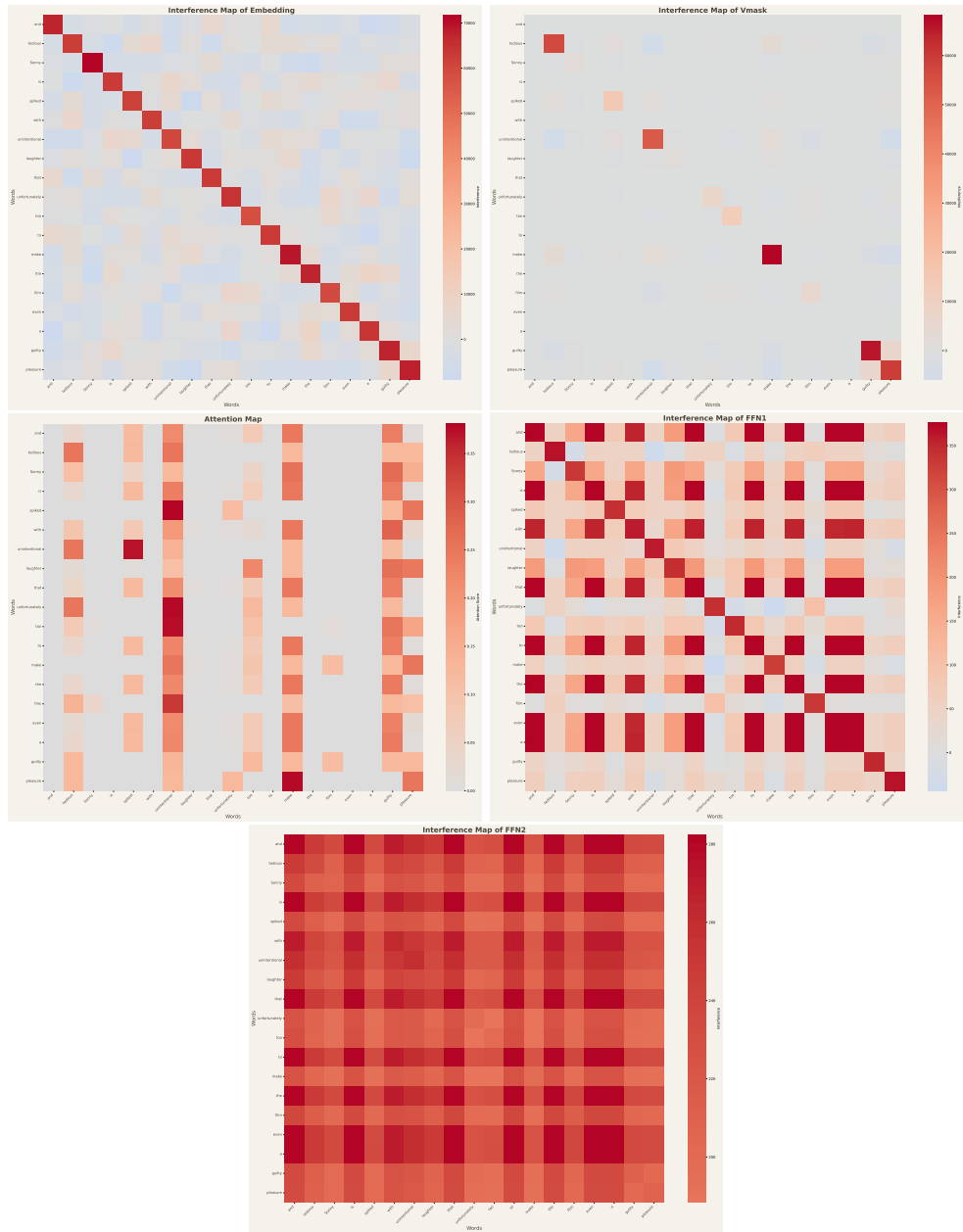


Figure 6: Cross Layers Output: Interference. Interference for FFN1 is interpretable.

Model	SST-2				IMDB			
	Acc _S	Acc _{$\tilde{S}^{(r)}$}	Acc _{$\tilde{S}^{(k)}$}	SRS	Acc _S	Acc _{$\tilde{S}^{(r)}$}	Acc _{$\tilde{S}^{(k)}$}	SRS
Baseline	71.81	75.81	74.96	-3.15	80.88	74.31	76.92	3.96
$\lambda_{Imp} = 0, \lambda_{Inter} = 0$	71.24	71.98	61.98	9.26	79.07	73.30	64.70	14.37
$\lambda_{Imp} = 0, \lambda_{Inter} = 0.01$	71.98	72.04	57.29	14.69	78.38	74.12	61.55	16.83
$\lambda_{Imp} = 0, \lambda_{Inter} = 1$	71.98	69.07	61.86	10.12	78.05	74.05	55.96	22.09
$\lambda_{Imp} = 0, \lambda_{Inter} = 100$	62.66	78.56	81.25	-18.59	77.19	72.60	64.46	12.73
$\lambda_{Imp} = 0.01, \lambda_{Inter} = 0$	73.47	69.70	59.35	14.12	78.63	74.48	50.42	28.21
$\lambda_{Imp} = 0.01, \lambda_{Inter} = 0.01$	74.10	73.13	62.78	11.32	78.23	74.52	51.19	27.04
$\lambda_{Imp} = 0.1, \lambda_{Inter} = 0.1$	72.78	70.67	60.43	12.35	77.64	74.06	50.05	27.59
$\lambda_{Imp} = 0.1, \lambda_{Inter} = 1$	73.87	74.27	60.38	13.49	76.88	73.38	50.02	26.86
$\lambda_{Imp} = 1, \lambda_{Inter} = 0$	71.47	72.16	55.35	16.12	74.93	71.57	50.00	24.93
$\lambda_{Imp} = 1, \lambda_{Inter} = 0.1$	72.96	75.30	54.72	18.24	73.64	70.72	50.00	23.64
$\lambda_{Imp} = 1, \lambda_{Inter} = 1$	71.58	73.70	56.89	14.69	74.10	70.89	50.00	24.10
$\lambda_{Imp} = 10, \lambda_{Inter} = 10$	70.84	73.24	57.00	13.84	60.73	58.73	50.00	10.73
$\lambda_{Imp} = 100, \lambda_{Inter} = 0$	59.86	64.95	51.57	8.29	52.04	51.81	50.09	1.95
$\lambda_{Imp} = 100, \lambda_{Inter} = 100$	61.46	62.04	51.06	10.40	51.80	51.72	50.00	1.80

Table 6: Ablation Study on SST-2 and IMDB datasets. λ choosing influence prediction accuracy and model interpretability.

D Regularization Hyperparameter Tuning

This section presents the results of hyperparameter tuning for λ_{Imp} and λ_{Inter} , as summarized in Table 6.